Self-organized criticality and pattern emergence through the lens of tropical geometry

N. Kalinin[a], A. Guzmán-Sáenz[b], Y. Prieto[c], M. Shkolnikov[d], V. Kalinina[e], and E. Lupercio[f,1]

[a]The Laboratory of Game Theory and Decision Making, National Research University Higher School of Economics, Saint-Petersburg 194100, Russia; [b]Computational Genomics, IBM T. J. Watson Research Center, Yorktown Heights, NY 10598; [c]Institut de Mathématiques de Toulouse, Université de Toulouse III Paul Sabatier, 31400 Toulouse, France; [d]Hausel Group, Institute of Science and Technology Austria, Klosterneuburg 3400, Austria; [e]Institute of Cytology, Russian Academy of Science, 194064 Saint-Petersburg, Russia; and [f]Department of Mathematics, CINVESTAV, Mexico City CP 07360, Mexico

Edited by Kenneth A. Ribet, University of California, Berkeley, CA, and approved July 13, 2018 (received for review April 4, 2018)

Tropical geometry, an established field in pure mathematics, is a place where string theory, mirror symmetry, computational algebra, auction theory, and so forth meet and influence one another. In this paper, we report on our discovery of a tropical model with self-organized criticality (SOC) behavior. Our model is continuous, in contrast to all known models of SOC, and is a certain scaling limit of the sandpile model, the first and archetypical model of SOC. We describe how our model is related to pattern formation and proportional growth phenomena and discuss the dichotomy between continuous and discrete models in several contexts. Our aim in this context is to present an idealized tropical toy model (cf. Turing reaction-diffusion model), requiring further investigation.

self-organized criticality | tropical geometry | proportional growth | power laws | pattern formation

The statistics concerning earthquakes in a particular extended region of the Earth during a given period obey a power law known as the Gutenberg–Richter law (1): The logarithm of the energy of an earthquake is a linear function of the logarithm of the frequency of earthquakes of such energy. An earthquake is an example of a dynamical system presenting both temporal and spatial degrees of freedom. The following definition generalizes these properties.

Definition 1. A dynamical system is a self-organized critical (SOC) system if it is slowly driven by an external force, exhibits avalanches, and has power law correlated interactions (cf. ref. 2, section 7).

By an avalanche, we mean a sudden recurrent modification of the internal energy of the system. In SOC systems, avalanches display scale invariance over energy and over time (2).*

Many ordinary critical phenomena near continuous phase transition (which requires fine tuning) display nontrivial power law correlations with a cutoff associated to the cluster size (4). For example, the Ising model shows power law correlations only for specific parameters, while an SOC system, behaving statistically in an analogous manner, achieves the critical state merely by means of a small external force, without fine-tuning.

The Sandpile Model

The concept of SOC was introduced in the seminal papers of Per Bak, Chao Tang, and Kurt Wiesenfeld (5, 6), where they put forward the archetypical example of an SOC system: the Sandpile Model. It is a highly idealized cellular automaton designed to display spatiotemporal scale invariance. Unlike other toy models in physics (e.g., the Ising model), a sandpile automaton does not attempt to apprehend the actual interactions of a physical system exhibiting SOC (such as a real sandpile). The sandpile cellular automaton is rather a mathematical model† that reproduces the statistical behavior of very diverse dynamical systems: It is descriptive at the level of global emergent phenomena without necessarily corresponding to such systems at the local reductionist level.

Imagine a large domain on a checkered plane; each vertex of this grid is determined by two integer coordinates (i,j). We will write $\mathbb{Z}^2$ to denote the integral square lattice formed by all pairs of integers (i,j) in the Euclidean plane $\mathbb{R}^2$. Our dynamical system will evolve inside Ω, which is the intersection of $\mathbb{Z}^2$ with a large convex figure in the plane. Throughout this paper, we use the word *graph* to indicate a collection of line segments (called edges) that connect points (called vertices) to each other.

Definition 2. A sandpile model consists of a grid inside a convex domain Ω on which we place grains of sand at each vertex; the number of grains on the vertex (i,j) is denoted by $\varphi(i,j)$ (see Fig. 1). Formally, a state is an integer-valued function $\varphi:\Omega\to\mathbb{Z}_{\geq 0}$. We call a vertex (i,j) unstable whenever there are four or more grains of sand at (i,j)—that is, whenever $\varphi(i,j)\geq 4$. The evolution rule is as follows: Any unstable vertex (i,j) topples spontaneously by sending one grain of sand to each of its four neighbors $(i,j+1),(i,j-1),(i-1,j),(i+1,j)$. The sand that falls outside Ω disappears from the system. Stable vertices cannot be toppled. Given an initial state φ, we will denote by φ° the stable state reached after all possible topplings have been performed. It is a remarkable and well-known fact that the final state φ° does not depend on the order of topplings. The final state φ° is called the relaxation of the initial state φ.

Bak and his collaborators proposed the following experiment: Take any stable state φ_0, and perturb it at random by adding

Significance

A simple geometric continuous model of self-organized criticality (SOC) is proposed. This model belongs to the field of tropical geometry and appears as a scaling limit of the classical sandpile model. We expect that our observation will connect the study of SOC and pattern formation to other fields (such as algebraic geometry, topology, string theory, and many practical applications) where tropical geometry has already been successfully used.

Author contributions: N.K., M.S., V.K., and E.L. designed research; N.K., A.G.-S., Y.P., M.S., V.K., and E.L. performed research; N.K., A.G.-S., Y.P., M.S., V.K., and E.L. analyzed data; and N.K., M.S., V.K., and E.L. wrote the paper.

The authors declare no conflict of interest.

This article is a PNAS Direct Submission.

Data deposition: The code and data have been deposited in https://github.com/elaldogs/tropicalsandpiles.

[1]To whom correspondence should be addressed. Email: elupercio@gmail.com.

Published online August 15, 2018.

*P. W. Anderson describes SOC as having "paradigmatic value" characterizing "the next stage of Physics." He writes: "In the 21^{st} century, one revolution which can take place is the construction of generalization which jumps and jumbles the hierarchies or generalizations which allow scale-free or scale transcending phenomena. The paradigm for the first is broken symmetry; for the second, self-organized criticality" (3).

†A holistic model in the sense of ref. 7.

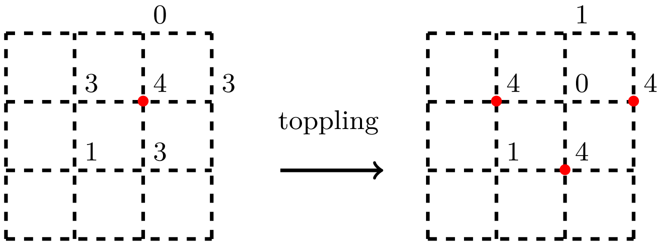

Fig. 1. Numbers represent the number of sand grains in the vertices of the grid, and a toppling is performed. Red points are unstable vertices.

a grain of sand at a random location. Denote the relaxation of the perturbed state by φ_1, and repeat this procedure. Thus, a sequence of randomly chosen vertices (i_k, j_k) gives rise to a sequence of stable states by the rule $\varphi_{k+1} = (\varphi_k + \delta_{i_k j_k})^\circ$.

The relaxation process $(\varphi_k + \delta_{i_k j_k}) \mapsto \varphi_{k+1}$ is called an avalanche[‡]; its size is the number of vertices that topple during the relaxation. Given a long enough sequence of uniformly chosen vertices (i_k, j_k), we can compute the distribution for the sizes of the corresponding avalanches. Let $N(s)$ be the number of avalanches of size s; then, the main experimental observation of ref. 5 is that

$$\log N(s) = \tau \log s + c.$$

In other words, the sizes of avalanches satisfy a power law. In Fig. 2, we have reproduced this result with $\tau \sim -1.2$. This has only very recently been given a rigorous mathematical proof using a deep analysis of random trees on the 2D integral lattice $\mathbb{Z}^2$ (8).

Definition 3. A recurrent state is a stable state appearing infinitely often, with probability one, in the above dynamical evolution of the sandpile.

Surprisingly, the recurrent states are exactly those which can be obtained as a relaxation of a state $\varphi \geq 3$ (pointwise). The set of recurrent states forms an Abelian group (9), and its identity exhibits a fractal structure in the scaling limit (Fig. 3); unfortunately, this fact has resisted a rigorous explanation so far.

The main point of this paper is to exhibit fully analogous phenomena in a continuous system (which is not a cellular automaton) within the field of tropical geometry.

An advantage of the tropical model is that, while it has SOC behavior, just as the classical model does, its states look much less chaotic; thus, we say that the tropical model has no combinatorial explosion.

Mathematical Modeling for Proportional Growth and Pattern Formation

The dichotomy between continuous mathematical models and discrete cellular automata has an important example in developmental biology.

A basic continuous model of pattern formation was offered by Alan Turing in 1952 (10). He suggested that two or more homogeneously distributed chemical substances, termed morphogens, with different diffusing rates and chemical activity, can self-organize into spatial patterns of different concentrations. This theory was confirmed decades later and can be applied, for example, to modeling the patterns of fish and lizard skin (11, 12) or of seashells' pigmentation (13).

On the discrete modeling side, the most famous model is the Game of Life developed by Conway in 1970 (14). A state of this 2D system consists of "live" and "dead" cells that function according to simple rules. Any live cell dies if there are fewer than two or more than three live neighbors. Any dead cell becomes alive if there are three live neighbors. A very careful control of the initial state produces "oscillators" and "spaceships" that certainly look fascinating but seem not to be related to realistic biological models. Nevertheless, a strong philosophical conclusion of the Game of Life is that extremely simple rules can produce behavior of arbitrary complexity. A more realistic cellular automaton has recently been derived from the continuous reaction-diffusion model of Turing. In ref. 15, the transformation of the juvenile white ocelli skin patterns of the lizard *Timon lepidus* into a green and black labyrinth was observed. In this study, the authors presented the skin squamae of lizard as a hexagonal grid, where the color of each individual cell depended on the color states of neighboring positions. This cell automaton could successfully generate patterns coinciding with those on the skin of adult lizards.

Pattern formation is related to an important problem in developmental biology: how to explain proportional growth. It is not clear why different parts of animal or human bodies grow at approximately the same rate from birth to adulthood. Sandpile simulations provide a qualitative toy model as follows.

Example 1. Early on, it was observed experimentally that sandpiles have fractal structure in their spatial degrees of freedom (see Fig. 4).

This example exhibits the phenomenon of proportional growth and scale invariance: If we rescale tiles to have area $\frac{1}{N}$ and let N go to infinity, then the picture converges in the weak-$\star$ sense. (See ref. 16 and references therein.) Recently, the patches and a linear pattern in this fractal picture were explained in refs. 17–19 using discrete superharmonic functions and Apollonian circle packing.

Dhar and Sadhu (20) established certain 2D sandpile models where the size of newly formed patterns depends on the number of sand grains added on the top, but the number and shape of the patterns remain the same. Strikingly, they also proposed a 3D model that also forms proportionally growing patterns; these patterns look like the head, thorax, and abdomen of real larva.

The perspective of our paper suggests that continuous tropical geometry should have consequences in the study of proportional growth modeling. We conjecture that tropical functions should appear as gradients of growth (compare figure 3 in ref. 21 and our Fig. 5; see also section 2.5 in ref. 22).

Tropical Geometry

Tropicalization can be thought of as the study of geometric and algebraic objects on the log–log scale[§] in the limit when the base of the logarithm is very large.[¶] Let us start by considering the most basic mathematical operations: addition and multiplication. With the logarithmic change of coordinates and with the base of the logarithm becoming infinitely large, multiplication becomes addition and addition becomes taking the maximum. Namely, define

$$x +_t y := \log_t(t^x + t^y)$$
$$x \times_t y := \log_t(t^x t^y)$$

for $x,\ y$ positive and then, taking the limit as t tends to $+\infty$, set

$$\mathrm{Trop}(x + y) := \lim_{t \to +\infty} x +_t y = \max(x, y),$$

$$\mathrm{Trop}(x \times y) := \lim_{t \to +\infty} x \times_t y = x + y.$$

[‡]We can think of an avalanche as an earthquake.

[§]Drawing algebraic varieties on log–log scale was successfully used by O. Ya. Viro, in his study of Hilbert's 17th problem, to construct real algebraic curves with prescribed topology; for a more recent account of this story, read ref. 23.

[¶]This limit has been discovered several times in physics and mathematics and was named Maslov dequantization in mathematical physics before it was called tropicalization in algebraic geometry (24).

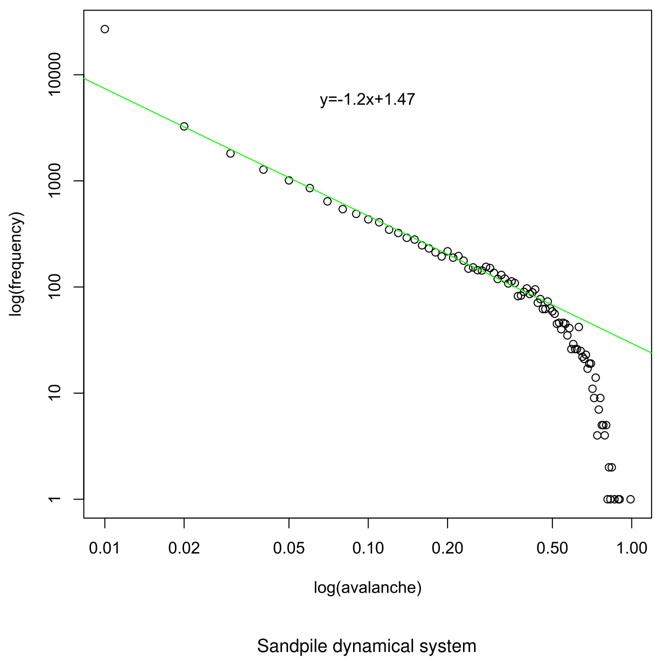

Fig. 2. The power law for sandpiles. The logarithm of the frequency is linear with respect to the logarithm of the avalanche size, except near the right where the avalanches are larger than half of the system. Here we have $\Omega = [0, 100]^2$ and is initially filled with three grains everywhere, followed by 106 dropped grains.

Tropical numbers are thus defined as the set of ordinary real numbers (together with $\{-\infty\}$; i.e., $\mathbb{T} := \mathbb{R} \cup \{-\infty\}$) and with tropical addition $\max(x, y)$ and multiplication $x + y$. The tropical numbers form a semiring: All of the usual rules of algebra hold in $\mathbb{T}$ with the exception of additive inverses (the neutral element for addition is $-\infty$; additive inverses are missing).

This mathematical structure simplifies some computations, and several optimization problems are solved efficiently in this way; this is a growing area of applied research in the current decade [it has been used in auctions for the Bank of England (25), for biochemical networks (26), and for Dutch railroads, among other things (27)].

Thermodynamics suggests that the tropical limit should be understood as the low temperature limit $T \to 0$ (or equivalently, as the limit when the Boltzmann constant k vanishes, $k \to 0$) of the classical algebraic and geometric operations. In this interpretation of the limit, the relevant change of variables is $t = e^{-\frac{1}{kT}}$, where t is the tropical parameter (the base of the logarithm) and T is the temperature (28–30). More relevant to realistic physical systems, tropical functions and tropical algebra appear naturally in statistical physics as the formal limit as $k \to 0$, and this can be used to analyze frustrated systems like spin ice and spin glasses. This is directly related to the appearance of the tropical degeneration in dimer models (28, 31).

Definition 4. Let $A \subset \mathbb{Z}^2$ be any finite set. A tropical polynomial in two variables is a function

$$\mathrm{Trop}(F(x, y)) = \max_{(i,j)\in\mathcal{A}} (a_{ij} + ix + jy). \qquad \textbf{[1]}$$

A tropical polynomial should be thought of the tropicalization of a classical polynomial $F(x, y) = \sum_{(i,j)\in A} a_{ij} x^i y^j$ obtained by replacing all of the summations and multiplications by their tropical counterparts—that is, $\max$ and addition, respectively.

For an excellent introduction to tropical geometry, we refer the reader to ref. 32.

Tropical Limit in Algebraic Geometry

Complex algebraic geometry is the field of mathematics that studies geometric objects inside complex Euclidean spaces $\mathbb{C}^n$ that arise as zero sets of finite families of polynomials. A simple example of such an object is an algebraic curve $\mathcal{C}$ given by a single polynomial equation in two variables

$$\mathcal{C} : F(x, y) = 0, \ \ (x, y) \in \mathbb{C}^2, F(x, y) = \sum_{(i,j)\in\mathcal{A}} a_{ij} x^i y^j.$$

Here $\mathcal{A}$ is a finite set of pairs of positive integers. The degree of F is the maximal total power $i + j$ of all of the monomials $x^i y^j$ appearing in F—namely, $d = \max_{(i,j)\in\mathcal{A}} (i + j)$. The curve $\mathcal{C}$ is a 2D object despite its name (for two real dimensions is the same as one complex dimension).

A nonsingular complex curve $\mathcal{C} = \{F(x, y) = 0\}$ of degree $d = \deg(F)$ is a Riemann surface of genus $g = \frac{1}{2}(d-1)(d-2)$. Therefore, the usual lines ($d = 1$) and quadrics ($d = 2$) are topological 2-spheres, while cubics ($d = 3$, also called elliptic curves), are tori.

The geometric counterpart of the tropicalization is as follows. Given a complex algebraic curve $\mathcal{C}_t$ defined by a polynomial

$$F_t(x, y) = \sum_{(i,j)\in\mathcal{A}} \gamma_{ij} t^{a_{ij}} x^i y^j = 0, |\gamma_{ij}| = 1,$$

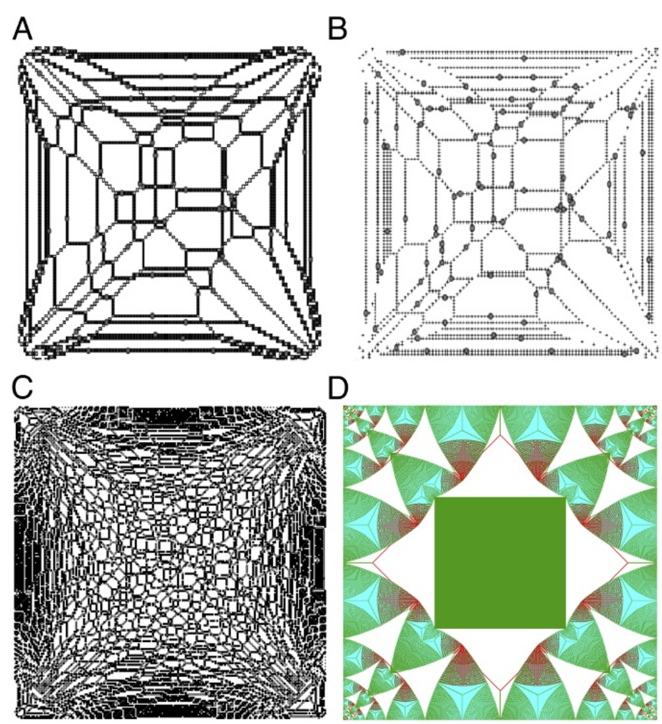

Fig. 3. The first two pictures show the comparison between the (*A*) classical and (*B*) tropical sandpiles for $|P| = 100$ generic points on the square. In *C*, the square Ω has side $N = 1000$; a large number ($|P| = 40000$) of grains has been added, showing the spatial SOC behavior on the tropical model compared with the identity (*D*) of the sandpile group on the square of side $N = 1000$. In the central square region on *C* (corresponding to the solid block of the otherwise fractal unit), we have a random tropical curve with edges on the directions (1, 0), (0, 1) and ($\pm$1, 1), which is given by a small perturbation of the coefficients of the tropical polynomial defining the usual square grid.

MATHEMATICS

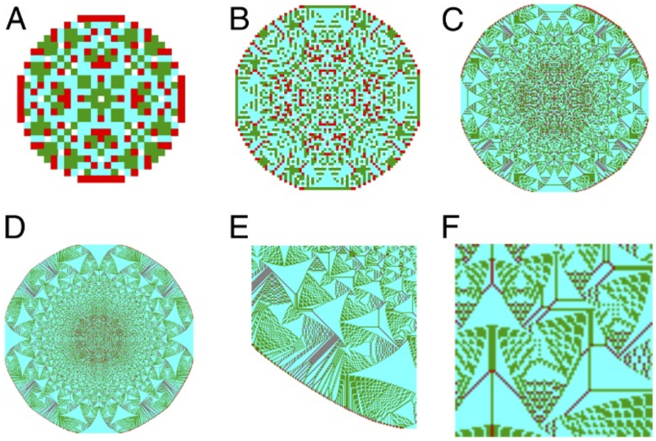

Fig. 4. In *A–D*, a very large number N of grains of sand is placed at the origin of the everywhere empty integral lattice; the final relaxed state shows fractal behavior. Here, as we advance from *A* to *D*, we see successive sandpiles for (*A*) $N=10^3$, (*B*) 10^4, (*C*) 10^5, and (*D*) 10^6, rescaled by factors of $\sqrt{N}$. In *E*, we zoom in on a small region of *D* to show its intricate fractal structure, and finally, in *F*, we further zoom in on a small portion of *E*. We can see proportional growth occurring in the patterns as the fractal limit appears. The balanced graphs inside the roughly triangular regions of *F* are tropical curves.

we call the amoeba A_t the image of $\mathcal{C}_t$ under the map $\log_t(x,y)=(\log_t|x|,\log_t|y|)$, $A_t:=\log_t(\mathcal{C}_t)$. The limit of the amoebas A_t as $t\to+\infty$ is called $\mathrm{Trop}(\mathcal{C})$, the tropicalization of $\mathcal{C}_t$.

The limit $\mathrm{Trop}(\mathcal{C})$ can be described entirely in terms of the tropical polynomial $\mathrm{Trop}(F)$ (Eq. **1**). This fact can be proved by noticing that on the linearity regions of $\mathrm{Trop}(F(x,y))$, one monomial in F_t dominates all of the others, and therefore, F_t cannot be zero, and consequently, we conclude that the limit $\mathrm{Trop}(\mathcal{C})$ is precisely the set of points (x,y) in the plane where the (3D) graph of the function

$$\mathrm{Trop}(F(x,y))=\max_{(i,j)\in\mathcal{A}}(a_{ij}+ix+jy)$$

is not smooth. This set of points is known as the corner locus of $\mathrm{Trop}(F(x,y))$. For this reason, we define the tropical plane curve as the corner locus of a tropical polynomial. As depicted in Fig. 6, the tropical degeneration $\mathrm{Trop}(\mathcal{C})$ of a complex curve $\mathcal{C}$ is essentially the graph of the curve depicted in a $\log_t-\log_t$ scale for t very large.

It is not very hard to verify that every tropical curve $\mathrm{Trop}(\mathcal{C})$ in the plane is a finite balanced graph, all of whose edges have rational slopes, such that at every vertex, the (weighted) directions of the primitive vectors in every direction cancel out (this is called the balancing condition and is akin to Kirchhoff's law for electrical circuits). Conversely, every such balanced graph on the plane appears as a tropical algebraic curve $\mathrm{Trop}(\mathcal{C})$. Here, it may be a good moment to point out that one can observe small tropical curves in Fig. 4, where the final state of a sandpile is depicted; this already points toward a relationship between SOC and tropical geometry.

String Theory, Mirror Symmetry

Tropical geometry is intimately related to the interaction between algebraic geometry and string theory that occurs in the mirror symmetry program. Given a tropical 2D surface B, we can use the tropical structure to produce a pair $(X_B,\tilde{X}_B)$ of mirror manifolds. This motivated M. Kontsevich to predict that counting tropical curves on B could be used for the calculation of Gromov–Witten invariants (which count holomorphic complex curves) in the A-side of mirror symmetry. The first example of such a calculation done from a rigorous mathematical perspective was accomplished by Mikhalkin (33). This perspective has been expanded by Gross and Siebert (34) in their program to understand mirror symmetry from a mathematical viewpoint using tropical geometry.

Let us also mention that the dichotomy between continuous and discrete models in our paper (already appearing in the biological models) has an important analogue in string theory: Iqbat et al. (35) have argued that, when we probe space–time beyond the scale α' and below Planck's scale, the resulting fluctuations of space–time can be computed with a classical cellular automaton (a melting crystal) representing quantum gravitational foam. Their theory is a three-tier system whose levels are classical geometry (Kähler gravity), tropical geometry (toric manifolds), and cellular automata (discrete melting crystals). The theory that we propose in this paper is also a three-tier system whose levels are classical complex algebraic geometry, tropical geometry (analytic tropical curves), and cellular automata (sandpiles). This seems not to be a coincidence and suggests deep connections between our model for SOC and their model for quantum gravitational foam.

Tropical Curves in Sandpiles

To understand the appearance of tropical geometry in sandpiles, consider the toppling function $H(i,j)$ defined as follows: Given an initial state φ and its relaxation φ°, the value of $H(i,j)$ equals the number of times that there was a toppling at the vertex (i,j) in the process of taking φ to φ°.

The discrete Laplacian of H is defined by the net flow of sand, $\Delta H(i,j):=$

$$H(i-1,j)+H(i+1,j)+H(i,j-1)+H(i,j+1)-4H(i,j).$$

The toppling function is clearly nonnegative on Ω and vanishes at the boundary. The function ΔH completely determines the final state φ° by the formula:

$$\varphi^\circ(i,j)=\varphi(i,j)+\Delta H(i,j). \quad \mathbf{[2]}$$

It can be shown by induction that the toppling function H satisfies the least action principle: If $\varphi(i,j)+\Delta F(i,j)\le 3$ is

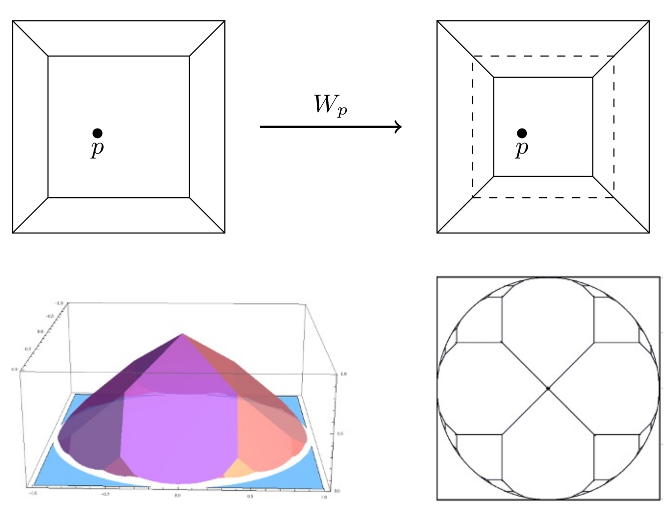

Fig. 5. (*Top*) The action of the wave operator W_p on a tropical curve. The tropical curve steps closer to p by an integral step. Thus, W_p shrinks the face to which p belongs; the combinatorial morphology of the face to which p belongs can actually change. (*Bottom*) The function $G_p\mathbf{0}$, where p is the center of the circle, and its associated omega-tropical curve are shown.

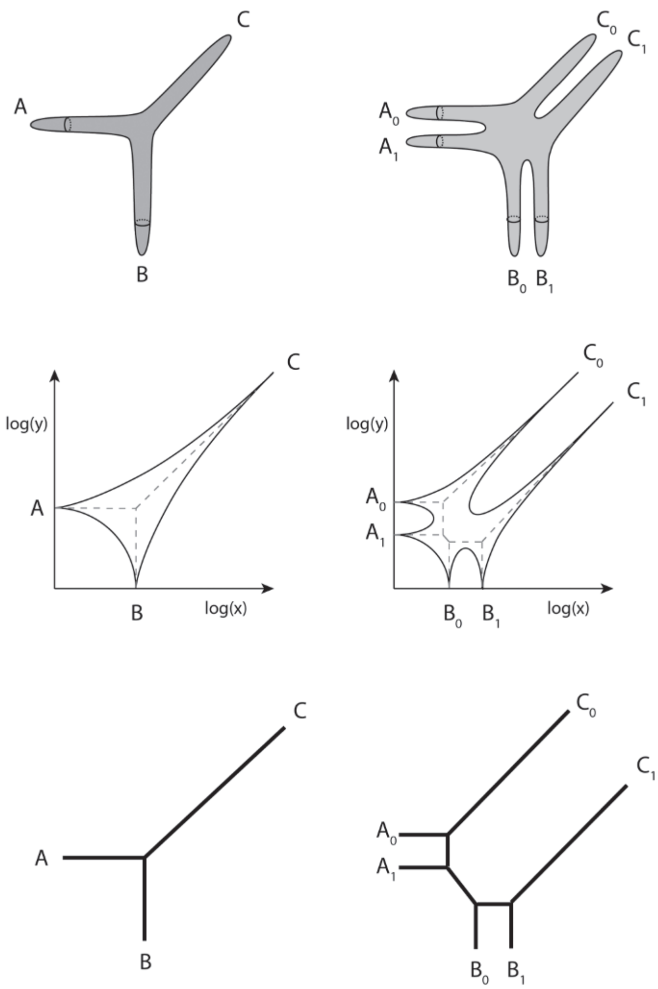

Fig. 6. Each column represents a tropical degeneration (from top to bottom). The complex picture is at the top; in the middle, we depict the amoeba on a log–log scale, and at the bottom, we picture the tropical curve that can be seen as the spine of the corresponding amoeba. In the first example, we have a degree-one curve with three points A, B, C going off to infinity [the intersections A, B of a line with the coordinate axes go to $-\infty$ under the logarithm, and C, the intersection at infinity, goes to $(+\infty, +\infty)$]. In the second example, a quadric degenerates sending six points off to infinity. A quadric intersects each of the coordinate lines and the line at infinity in two points; therefore, six (three times two) points go off to infinity. From top to bottom, $t \to \infty$.

stable, then $F(i,j) \geq H(i,j)$. Ostojic (36) noticed that $H(i,j)$ is a piecewise quadratic function in the context of example 1.

Consider a state φ, which consists of three grains of sand at every vertex, except at a finite family of points

$$P = \{p_1 = (i_1, j_1), \dots, p_r = (i_r, j_r)\}$$

where we have four grains of sand:

$$\varphi := \langle 3 \rangle + \delta_{p_1} + \dots + \delta_{p_r} = \langle 3 \rangle + \delta_P. \qquad [3]$$

The state φ° and the evolution of the relaxation can be described by means of tropical geometry [the final picture (D) of Fig. 7 is a tropical curve]. This was discovered by Caracciolo et al. (37), while a rigorous mathematical theory to prove this fact has been given by Kalinin et al. (38), which we review presently. It is a remarkable fact that, in this case, the toppling function $H(i,j)$ is piecewise linear (after passing to the scaling limit).

To prove this, one considers the family $\mathcal{F}_P$ of functions on Ω that are (*i*) piecewise linear with integral slopes, (*ii*) nonnegative over Ω and zero at its boundary, (*iii*) concave, and (*iv*) not smooth at every point p_i of P. Let F_P be the pointwise minimum of functions in $\mathcal{F}_P$. Then, $F_P \geq H$ by the Least Action Principle [since $\Delta F_P \leq 0, \Delta F_P(p_i) < 0$].

Lemma 1. In the scaling limit, $H = F_P$.

A sketch of a proof. We introduce the wave operators W_p (39, 40) at the cellular automaton level and the corresponding tropical wave operators G_p. Given a fixed vertex $p = (i_0, j_0)$, we define the wave operator W_p acting on states φ of the sandpile as:

$$W_p(\varphi) := (T_p(\varphi + \delta_p) - \delta_p)^\circ,$$

where T_p is the operator that topples the state $\varphi + \delta_p$ at p once, if it is possible to topple p at all. In a computer simulation, the application of this operator looks like a wave of topplings spreading from p, while each vertex topples at most once.

The first important property of W_p is that, for the initial state $\varphi := \langle 3 \rangle + \delta_P$, we can achieve the final state φ° by successive applications of the operator $W_{p_1} \circ \dots \circ W_{p_r}$ a large but finite number of times (despite the notation):

$$\varphi^\circ = (W_{p_1} \cdots W_{p_r})^\infty \varphi + \delta_P.$$

This process decomposes the total relaxation $\varphi \mapsto \varphi^\circ$ into layers of controlled avalanching.

The second important property of the wave operator W_p is that its action on a state $\varphi = \langle 3 \rangle + \Delta f$ has an interpretation in

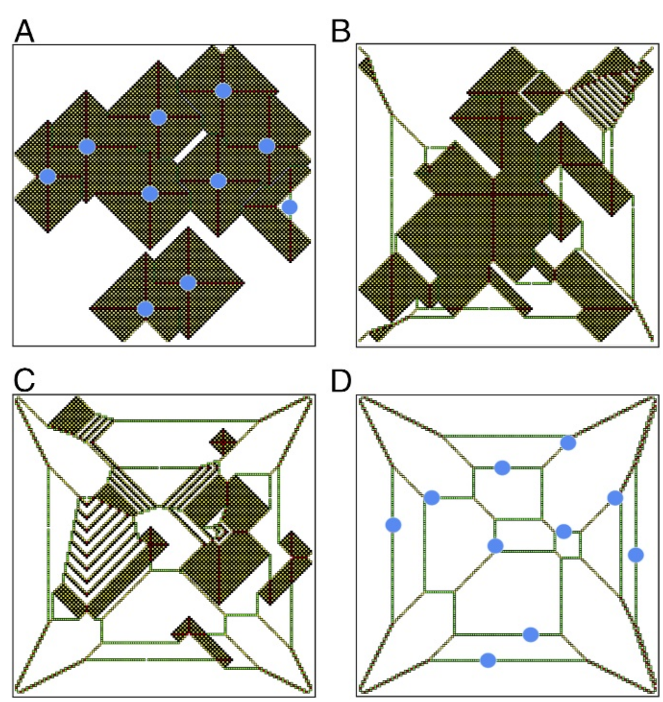

Fig. 7. The evolution of $\langle 3 \rangle + \delta_P$. Sand falling outside the border disappears. Time progresses in the sequence A, B, C, and finally D. Before A, we add grains of sand to several points of the constant state $\langle 3 \rangle$ (we see their positions as blue disks given by δ_P). Avalanches ensue. At time A, the avalanches have barely started. At the end, at time D, we get a tropical analytic curve on the square Ω. White represents the region with three grains of sand, while green represents two, yellow represents one, and red represents the zero region. We can think of the blue disks δ_P as the genotype of the system, of the state $\langle 3 \rangle$ as the nutrient environment, and of the thin graph given by the tropical function in D as the phenotype of the system.

terms of tropical geometry. To wit, whenever f is a piecewise linear function with integral slopes that, in a neighborhood of p, is expressed as $a_{i_0j_0} + i_0x + j_0y$, we have

$$W_p(\langle 3\rangle + \Delta f) = \langle 3\rangle + \Delta\, W(f),$$

where $W(f)$ has the same coefficients a_{ij} as f except one—namely, $a'_{i_0j_0} = a_{i_0j_0} + 1$. This is to account for the fact that the support of the wave is exactly the face where $a_{i_0j_0} + i_0x + j_0y$ is the leading part of f.

We will write $G_p := W_p^{\infty}$ to denote the operator that applies W_p to $\langle 3\rangle + \Delta f$ until p lies in the corner locus of f. We repeat that it has an elegant interpretation in terms of tropical geometry: G_p increases the coefficient $a_{i_0j_0}$ corresponding to a neighborhood of p, lifting the plane lying above p in the graph of f by integral steps until p belongs to the corner locus of G_pf. Thus, G_p has the effect of pushing the tropical curve toward p (Fig. 5) until it contains p.

From the properties of the wave operators, it follows immediately that

$$F_P = (G_{p_1} \cdots G_{p_r})^{\infty}\mathbf{0},$$

where $\mathbf{0}$ is the function that is identically zero on Ω. All intermediate functions $(G_{p_1} \cdots G_{p_r})^k\mathbf{0}$ are less than H since they represent partial relaxations, but their limit belongs to $\mathcal{F}_P$, and this, in turn, implies that $H = F_P$.

Conclusion. We have shown that the toppling function H for Eq. **3** is piecewise linear. Thus, applying Eq. **2**, we obtain that φ° is equal to 3 everywhere but the locus where $\Delta H \neq 0$—that is, its corner locus, namely an Ω-tropical curve (Fig. 7).

Definition 5. An Ω-tropical series is a piecewise linear function on Ω given by

$$F(x, y) = \min_{(i,j)\in\mathcal{A}} (a_{ij} + ix + jy),$$

where the set $\mathcal{A}$ is not necessarily finite and $F|_{\partial\Omega} = 0$ (41). An Ω-tropical curve is the set where F is not smooth. Each Ω-tropical curve is a locally finite graph satisfying the balancing condition.

Remark 1. Tropical curves consist of edges, such that to each direction of the edges there corresponds a line-shaped pattern (a string) such as the one encountered in Fig. 4; these patterns can be computed (18). In simulations, we have observed that these strings act like the renormalization group and, thus, ensure the proportional growth of the quadratic patches in Fig. 4. The same occurs in other sandpile models with proportional growth, which suggests that tropical geometry is a less reductionist tool than cellular automata to study this phenomenon.

The Tropical Sandpile (TS) Model

Here, we define a model, the TS, reflecting structural changes when a sandpile evolves. The definition of this dynamical system is inspired by the mathematics of the previous section; TS is not a cellular automaton, but it exhibits SOC.

The dynamical system lives on the convex set $\Omega = [0, N] \times [0, N]$; we will consider Ω to be a very large square. The input data of the system are a large but finite collection of points $P = \{p_1, \ldots, p_r\}$ with integer coordinates on the square Ω. Each state of the system is an Ω-tropical series (and the associated Ω-tropical curve).

The initial state for the dynamical system is $F_0 = \mathbf{0}$, and its final state is the function F_P defined previously. Notice that the definition of $\mathcal{F}_P$, while inspired by sandpile theory, uses no sandpiles or cellular automata whatsoever. Intermediate states $\{F_k\}_{k=1,\ldots,r}$ satisfy the property that F_k is not smooth at $p_1, p_2, \ldots, p_k$; that is, the corresponding tropical curve passes through these points.

In other words, the tropical curve is first attracted to the point p_1. Once it manages to pass through p_1 for the first time, it continues to try to pass through $\{p_1, p_2\}$. Once it manages to pass through $\{p_1, p_2\}$, it proceeds in the same manner toward $\{p_1, p_2, p_3\}$. This process is repeated until the curve passes through all of $P = \{p_1, \ldots, p_r\}$.

We will call the modification $F_{k-1} \to F_k$ the kth avalanche. It occurs as follows: To the state F_{k-1} we apply the tropical operators $G_{p_1}, G_{p_2}, \ldots, G_{p_k}; G_{p_1}, \ldots$ in cyclic order until the function stops changing; the discreteness of the coordinates of the points in P ensures that this process is finite.[‖] Again, as before, while sandpile-inspired, the operators G_p are defined entirely in terms of tropical geometry without mention of sandpiles.

There is a dichotomy: Each application of an operator G_p either does something to change the shape of the current tropical curve (in this case, G_p is called an active operator) or does nothing, leaving the curve intact (if p already belongs to the curve).

Definition 6. The size of the kth avalanche is the number of distinct active operators G_{p_i} used to take the system from the self-critical state F_{k-1} to the next self-critical state F_k, divided by k. In particular, the size s_k of the kth avalanche is a number between 0 and 1, $0 \leq s_k \leq 1$, and it estimates the proportional area of the picture that changed during the avalanche.

In the previous example, as the number of points in P grows and becomes comparable to the number of lattice points in Ω, the TS exhibits a phase transition going into spatial SOC (fractality). This provides evidence in favor of SOC on the TS model, but there is a far more subtle spatiotemporal SOC behavior that we will exhibit in the following paragraphs.

While the ordering of the points from the first to the rth is important for the specific details of the evolution of the system, the system's statistical behavior and final state are insensitive to it. This is called an Abelian property, which was studied extensively in ref. 42 for discrete dynamical systems (Abelian networks). Our model suggests studying continuous dynamical systems with this Abelian property, such as, for example, Abelian networks with nodes on the plane, a continuous set of states, and an evolution rule depending on the coordinates of the nodes. We expect that the Abelian property is equivalent to the least action principle (cf. ref. 42).

SOC in the Tropical World

The TS dynamics exhibit slow driving avalanching (in the sense of ref. 2, p. 22).

Once the tropical dynamical system stops after r steps, we can ask ourselves what the statistical behavior of the number $N(s)$ of avalanches of size s is like. We posit that the tropical dynamical system exhibits spatiotemporal SOC behavior; that is, we have a power law:

$$\log N(s) = \tau \log s + c.$$

To confirm this, we have performed experiments in the supercomputing clusters ABACUS and Xiuhcoatl at Cinvestav (Mexico City); the code is available at https://github.com/elaldogs/tropicalsandpiles. In Fig. 8, we see the graph of $\log N(s)$ vs. $\log s$ for the tropical (piecewise linear, continuous) sandpile dynamical system; the resulting experimental τ in this case was $\tau \sim -0.9$.

Conclusion and Further Directions

We have obtained a piecewise-linear (continuous, tropical) model to study statistical aspects of nonlinear phenomena. As

‖ If the coordinates of the points in P are not integers, the model is well-defined, but we need to take a limit (see ref. 41), which is not suitable for computer simulations.

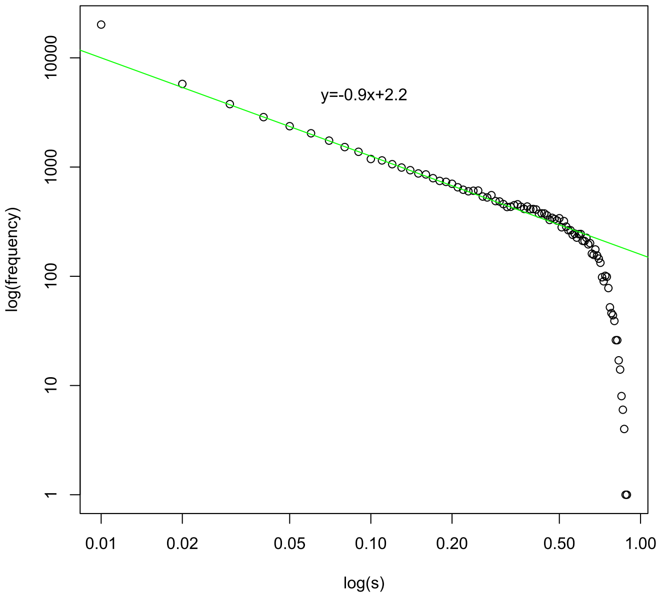

Fig. 8. The power law for the tropical (piece-wise linear, continuous) dynamical system. In this computer experiment, Ω has a side of 1,000 units, and we add at random a set P of 10,000 individual sand grains (a random large genotype).

tropical geometry is highly developed, it seems reasonable to believe that it will provide new reductionist explanations for physical nonlinear systems in the future (as well as providing a tool for studying proportional growth phenomena in biology and elsewhere), as has already happened with nonlinear aspects of algebraic geometry and mirror symmetry.

Next, we list open questions.

From the point of view of real physical phenomena, the TS provides a class of mathematical and modeling tools. Some possible directions for further research are as follows:

Direction 1. If Ω is a polygon with sides of rational slope, then each Ω-tropical curve C can be obtained as the corner locus of F_P for a certain set P of points. To achieve this, one considers a (finite) set P of points that all belong to C and cover C rather densely, meaning that every point in C is very close to a point in P (at a distance less than a very small ϵ). As is shown in ref. 41, the corner locus of F_P is an Ω-tropical curve passing through P that solves a certain Steiner-type problem: minimizing the tropical symplectic area. However, because the set P is huge in this construction, an open question remains: Can we find a small set $P=\{p_1,\dots,p_r\}$ (where r is approximately equal to the number of faces of C) such that C is the corner locus of F_P? (We thank an anonymous referee for this question.)

Direction 2. The operators G_p can be lifted to the algebraic setting, but for now, we can do this only in fields of characteristic two (41). Is it possible to lift G_p in characteristic zero (the complex realm)? In any case, we expect that this difficulty can be alleviated by a mirror symmetry interpretation. The issue is due to the symplectic nature of G_p: Indeed, Ω-tropical curves naturally appear as tropical symplectic degenerations (43, 44). When Ω is not a rational polygon, one should take into account noncommutative geometry (45). What is the mirror analog of G_p in the complex world? We expect that there should exist an operator G_p^* acting on strings, and through this we expect power-law statistics for a mirror notion of the areas of the faces of Ω-tropical curves.

Closely related to this, in analogy to the work of Iqbar et al. (35), we conjecture that the partition function obtained by summing over statistical mechanical configurations of sandpiles should have, via mirror symmetry, an interpretation as a path integral in terms of Kähler geometry. Tropical geometry should play the role of toric geometry in this case. What is the precise geometric model in this situation?

Developments in this direction would allow a new renormalization group interpretation of SOC (cf. refs. 46 and 47).

Direction 3. Rastelli and Känel studied nanometer-sized 3D islands formed during epitaxial growth of semiconductors appearing as faceted pyramids that seem to be modeled by tropical series from an inspection of Fig. 5 in this paper and figure 3 in ref. 21. It would be very interesting to prove that this is so and to study the consequences of this observation to the modeling of the morphology of such phenomena.

This may not be totally unrelated to allometry in biology. Is it possible that the gradient slope model, as in section 2.5 in ref. 22, could be piecewise linear, and the corner locus slopes could prescribe the type and speed of growth for tissues?

Direction 4. Study the statistical distributions for the coefficients of the tropical series in Fig. 3*C*. Explain why the slopes are mostly of directions $(0,1),(1,0),(1,1),(-1,1)$. Is it possible that a concentration measure phenomenon takes place and that such a type of picture appears with probability one? (We thank Lionel Levine for this question.)

Experimental Data

The data used to produce Figs. 2 and 8 can be found at https://github.com/elaldogs/tropicalsandpiles.

ACKNOWLEDGMENTS. N.K. was funded by Swiss National Science Foundation PostDoc.Mobility Grant 168647, supported in part by a Young Russian Mathematics award, and Grant FORDECYT-265667 "Programa para un Avance Global e Integrado de la Matemática Mexicana." Also, support from the Basic Research Program of the National Research University Higher School of Economics is gratefully acknowledged. Y.P. was funded by Grant FORDECYT-265667 and by "ABACUS" Laboratorio de Matemática Aplicada y Cómputo de Alto Rendimiento CINVESTAV-EDOMEX Proyecto CONACYT-EDOMEX-2011-01-165873 (Cinvestav). M.S. was supported by an Institute of Science and Technology Postdoctoral Fellowship program. E.L. thanks the Moshinsky Foundation, Conacyt, FORDECYT-265667, "ABACUS" Laboratorio de Matemática Aplicada y Cómputo de Alto Rendimiento CINVESTAV-EDOMEX Proyecto CONACYT- EDOMEX-2011-01-165873, Xiuhcoatl, Instituto de Matemáticas de la Universidad Nacional Autonoma de México, Samuel Gitler International Collaboration Center and the Laboratory of Mirror Symmetry National Research University Higher School of Economics, Russian Federation Government Grant 14.641.31.0001, and the kind hospitality of the University of Geneva and of the Mathematisches Forschungsinstitut Oberwolfach, where this work started.

1. Newman ME (2005) Power laws, pareto distributions and zipf's law. *Contemp Phys* 46:323–351.
2. Watkins NW, Pruessner G, Chapman SC, Crosby NB, Jensen HJ (2016) 25 years of self-organized criticality: Concepts and controversies. *Space Sci Rev* 198:3–44.
3. Anderson PW (2011) *More and Different: Notes from a Thoughtful Curmudgeon* (World Scientific, Singapore).
4. Aharony A, Stauffer D (2003) *Introduction to Percolation Theory* (Taylor & Francis, London).
5. Bak P, Tang C, Wiesenfeld K (1987) Self-organized criticality: An explanation of the 1/f noise. *Phys Rev Lett* 59:381–384.
6. Bak P, Tang C, Wiesenfeld K (1988) Self-organized criticality. *Phys Rev A* 38:364–374.
7. Downey AB (2012) *Think Complexity: Complexity Science and Computational Modeling* (O'Reilly Media, Inc., Boston).
8. Bhupatiraju S, Hanson J, Járai AA (2017) Inequalities for critical exponents in *d*-dimensional sandpiles. *Electron J Probab* 22:85.
9. Dhar D (1990) Self-organized critical state of sandpile automaton models. *Phys Rev Lett* 64:1613–1616.
10. Turing AM (1952) The chemical basis of morphogenesis. *Philos Trans R Soc Lond B: Biol Sci* 237:37–72.

MATHEMATICS

11. Kondo S, Asai R (1995) A reaction–diffusion wave on the skin of the marine angelfish pomacanthus. *Nature* 376:765–768.
12. Dhillon DSJ, Milinkovitch MC, Zwicker M (2017) Bifurcation analysis of reaction diffusion systems on arbitrary surfaces. *Bull Math Biol* 79:788–827.
13. Fowler DR, Meinhardt H, Prusinkiewicz P (1992) Modeling seashells. *ACM SIGGRAPH Computer Graphics*, ed Thomas JJ (ACM, New York), Vol 26, pp 379–387.
14. Gardner M (1970) Mathematical games: The fantastic combinations of John Conway's new solitaire game "life". *Sci Am* 223:120–123.
15. Manukyan L, Montandon SA, Fofonjka A, Smirnov S, Milinkovitch MC (2017) A living mesoscopic cellular automaton made of skin scales. *Nature* 544:173–179.
16. Pegden W, Smart CK (2013) Convergence of the Abelian sandpile. *Duke Math J* 162:627–642.
17. Levine L, Pegden W, Smart CK (2016) Apollonian structure in the Abelian sandpile. *Geom Funct Anal* 26:306–336.
18. Kalinin N, Shkolnikov M (2017) Sandpile solitons via smoothing of superharmonic functions. arXiv:1711.04285.
19. Levine L, Pegden W, Smart CK (2017) The Apollonian structure of integer superharmonic matrices. *Ann Math* 186:1–67.
20. Dhar D, Sadhu T (2013) A sandpile model for proportionate growth. *J Stat Mech Theor Exp* 2013:P11006.
21. Rastelli A, von Känel H (2002) Surface evolution of faceted islands. *Surf Sci* 515:L493–L498.
22. Vollmer J, Casares F, Iber D (2017) Growth and size control during development. *Open Biol* 7:170190.
23. Viro O (2006) Patchworking real algebraic varieties. arXiv preprint math/0611382.
24. Kolokoltsov V, Maslov VP (1997) *Idempotent Analysis and Its Applications* (Springer Science & Business Media, Dordrecht, The Netherlands), Vol 401.
25. Klemperer P (2010) The product-mix auction: A new auction design for differentiated goods. *J Eur Econ Assoc* 8:526–536.
26. Radulescu O, Gorban AN, Zinovyev A, Noel V (2012) Reduction of dynamical biochemical reactions networks in computational biology. *Front Genet* 3:131.
27. Heidergott B, Olsder GJ, Van der Woude J (2014) *Max Plus at Work: Modeling and Analysis of Synchronized Systems: A Course on Max-Plus Algebra and its Applications* (Princeton Univ Press, Princeton).
28. Kenyon R, Okounkov A, Sheffield S (2006) Dimers and amoebae. *Ann Math* 163:1019–1056.
29. Kapranov M (2011) Thermodynamics and the moment map. arXiv:1108.3472.
30. Itenberg I, Mikhalkin G (2012) Geometry in the tropical limit. *Mathematische Semesterberichte* 59:57–73.
31. Cimasoni D, Reshetikhin N (2007) Dimers on surface graphs and spin structures. i. *Commun Math Phys* 275:187–208.
32. Maclagan D, Sturmfels B (2015) *Introduction to Tropical Geometry, Graduate Studies in Mathematics* (American Mathematical Society, Providence, RI), Vol 161, pp xii+363.
33. Mikhalkin G (2005) Enumerative tropical algebraic geometry in $\mathbb{R}^2$. *J Amer Math Soc* 18:313–377.
34. Gross M (2011) Tropical geometry and mirror symmetry. *CBMS Regional Conference Series in Mathematics* (American Mathematical Society, Providence, RI), Vol 114, pp xvi+317.
35. Iqbal A, Vafa C, Nekrasov N, Okounkov A (2008) Quantum foam and topological strings. *J High Energy Phys* 2008:011–011.
36. Ostojic S (2003) Patterns formed by addition of grains to only one site of an abelian sandpile. *Physica A Stat Mech Appl* 318:187–199.
37. Caracciolo S, Paoletti G, Sportiello A (2010) Conservation laws for strings in the abelian sandpile model. *EPL (Europhys Lett)* 90:60003.
38. Kalinin N, Shkolnikov M (2016) Tropical curves in sandpile models. arXiv:1502.06284.
39. Ivashkevich EV, Ktitarev DV, Priezzhev VB (1994) Waves of topplings in an Abelian sandpile. *Physica A Stat Mech Appl* 209:347–360.
40. Ktitarev D, Lübeck S, Grassberger P, Priezzhev V (2000) Scaling of waves in the Bak-Tang-Wiesenfeld sandpile model. *Phys Rev E* 61:81–92.
41. Kalinin N, Shkolnikov M (2016) Introduction to tropical series and wave dynamic on them. arXiv:1706.03062.
42. Bond B, Levine L (2016) Abelian networks I. Foundations and examples *SIAM J Discrete Math* 30:856–874.
43. Mikhalkin G (2018) Examples of tropical-to-Lagrangian correspondence. arXiv: 1802.06473.
44. Matessi D (2018) Lagrangian pairs of pants. arXiv:1802.02993.
45. Katzarkov L, Lupercio E, Meersseman L, Verjovsky A (2014) The definition of a non-commutative toric variety. *Algebraic Topology: Appl New Dir* 620:223–250.
46. Diaz-Guilera A (1994) Dynamic renormalization group approach to self-organized critical phenomena. *EPL (Europhys Lett)* 26:177–182.
47. Ansari MH, Smolin L (2008) Self-organized criticality in quantum gravity. *Classical Quan Gravity* 25:095016.